Sub-40 fs optical parametric oscillator beyond the gain bandwidth limit

ABDULLAH ALABBADI,* **TOBIAS STEINLE, AND HARALD GIESSEN**

4th Physics Institute, University of Stuttgart, Pfaffenwaldring 57, 70569 Stuttgart, Germany
Corresponding author: abbadi@alexu.edu.eg

We report a compact and passively stable optical parametric oscillator for direct generation of sub-40 fs pulses, five times shorter than the 200 fs pump oscillator. By employing an intracavity all normal dispersion feedback fiber, we achieved low-noise and coherent broadening beyond the parametric gain bandwidth limitation. We demonstrate spectral coverage from 1.1 to 2.0 μm with excellent passive power and spectral stability below 0.1% rms and a footprint smaller than 14 × 14 cm². © 2022 Optica Publishing Group

https://doi.org/10.1364/OL.462085

Single-cycle pulse generation has been an important task in the last decade in the field of laser physics. Applications in ultrafast spectroscopy require pulses that explore this ultimate temporal limit in different spectral ranges. After initial demonstration of 6.7 fs pulses using a dye laser [1] and sub-10 fs pulse in Ti-sapphire lasers [2,3], more sophisticated methods of broadband pulse synthesis and subsequent compression came along, which led to pulse duration in the near-IR as short as single cycles using an Er-doped fiber laser, with broadening in several highly nonlinear fibers, and recompression using prisms [4]. Often, fiber lasers and their ultrabroadened spectra suffer from noise that is due to the amplified spontaneous emission processes in the rather long fiber gain medium. Alternative approaches include solid-state pump lasers, which give shot-noise limited performance above 300 kHz, owing to their short-gain crystals. To achieve tunable ultrashort few-cycle pulses in the near- and mid-IR, optical parametric oscillators (OPOs) are required.

Hebling *et al.* [5] obtained 34-fs pulses in a 2 mm potassium titanyl phosphate (KTP) OPO, pumped by a 26-fs Ti-sapphire laser. In the mid-IR, 36-fs pulses were achieved by using the idler of a 250 μm thick periodically poled lithium niobate (PPLN) crystal pumped by a 20 fs Ti-sapphire oscillator [6]. Enhancement of the signal bandwidth was also demonstrated by taking advantage of self-phase modulation (SPM) in a ZnSe plate in the cavity [7]. In the mentioned examples, free-space OPOs have been used, which suffer from stability, cavity length stabilization, and space issues, especially in the case of sub-30 fs pulses and repetition rates lower than 80 MHz. Recently, fiber-feedback OPOs have proven to be extremely robust, compact, and stable sources for tunable near- and mid-IR radiation [8–12]. However, so far, the shortest pulses obtained by drawing on this elegant concept were only 80 fs [12].

Fig. 1. Broadband fiber-feedback OPO. The driving pulses from a mode-locked pump laser are sent through a DM and focused with a 33 mm focal-length gold coated off-axis parabolic mirror (OAP) onto the nonlinear crystal. The generated signal beam is collimated with a similar OAP and then coupled into the nonlinear FF with a 12 mm focal-length achromatic collimating lens (C). The SPM-enhanced signal beam is coupled out by utilizing a combination of a polarizing beam splitter (PBS) and a quarter-wave plate (QWP) acting as a variable outcoupler. Temporal compression is subsequently realized using a 150 lines/mm grating pair compressor. M_1–M_5, gold coated mirrors; HWP, half-wave plate. The footprint of the fiber-feedback OPO is 14 × 14 cm².

Here, we break the 40-fs barrier, introducing a normal dispersion feedback fiber (FF) and external grating compression for a fiber-feedback OPO. We demonstrate 36 fs and 38 fs pulses that can be tuned across the 1.25–2.0 μm spectral range. We demonstrate excellent power and spectral stability without external stabilization lower than 0.1% rms over 2 h and shot noise limited performance above 300 kHz.

The driving pump pulses are produced by a Yb-based mode-locked oscillator (Flint, Light Conversion) with 76 MHz repetition rate, central wavelength of 1.03 μm, and 200 fs pulse duration (assuming Gaussian shape) measured before the nonlinear crystal. After passing through an optical isolator and power

regulator (PBS$_1$ + HWP), these pulses were coupled to an optical cavity through a dichroic mirror (DM). The cavity consists of two arms; the first arm is used for beam shaping and the second arm is for cavity length tuning and outcoupling (see Fig. 1). Both arms are optically connected with a 1 m single-mode fiber consisting of 0.86 m UHNA7 (Coherent-Nufern) spliced to 0.14 m SMF-28. In the first arm, the pump beam is focused onto a 5 mm PPLN crystal to a focal spot diameter of 25 μm (1/e^2 intensity). The nonlinear crystal has nine poling periods in the range 27–31 μm, enabling signal pulses that are tunable from 1.35 μm to 2 μm. The crystal is antireflection coated for pump, signal, and idler wavelengths and operated at room temperature (20–25°C) with no temperature control. The generated signal beam is collimated after the crystal, reflected by DM$_2$, and fed back into the fiber to reach the second arm. The idler and remaining pump are transmitted through DM$_2$ into a beam dump. The second arm consists of a variable outcoupler (PBS$_2$ + QWP), and a gold mirror mounted on a translation stage acting as a delay to achieve synchronization between the pump and signal pulses. It is essential to reduce the coupling losses from the first arm to the second arm where outcoupling takes place. The UHNA7 fiber has a mode field diameter (MFD) of only 3.2 μm (at 1550 nm), resulting in challenging coupling [13]. However, by splicing it to a larger MFD fiber (such as SMF μm at 1550 nm), we achieved up to ∼70% launching efficiency and significantly reduced coupling sensitivity. The splice transmission was maximized to 95% by employing the thermal expanding core technique [13]. In addition to its key feature of enabling an ultracompact architecture, this fiber-feedback approach has an essential advantage for pointing stability by decoupling cavity length tuning arm from beam shaping arm. This facilitates fast and stable tunability [14].

A key parameter limiting the parametric gain bandwidth of ultrafast OPOs is the nonlinear crystal thickness [15,16]. When the signal pulses were outcoupled after the nonlinear crystal, −20 dB bandwidths of only 40–60 nm were achieved. However, this limitation does not apply to $\chi^{(3)}$ nonlinearity. A spectral coverage of up to 600 nm (−20 dB), as shown in Fig. 2, was achieved by taking advantages of SPM in the FF. When the

fiber-feedback OPO was pumped by 900 mW, and by combining phase matching in the nonlinear crystal and SPM in the FF, tunable ultrabroad spectra were achieved covering 1.1–2 μm by changing the poling periods, as illustrated in Fig. 2(a). The spectra were up to 12 times wider (−20 dB) when SPM enhanced the operation in comparison with regular operation if relying only on the parametric gain bandwidth. Additionally, the spectral broadening could be controlled by adjusting the intracavity power launched into the fiber by changing either the outcoupling ratio or the pump power. Figure 2(b) shows the spectral broadening from 55 nm to 430 nm when increasing the pump power from 300 mW to 900 mW at a fixed grating period of 29 μm. The maximum pump power is mainly limited by the damage threshold of the nonlinear crystal. The available signal power was in the range of 60–90 mW and higher values could be achieved by enhancing the coupling efficiency into the fiber from the first arm. To reach a suitable power level for sufficient broadening in the spectral region above 1800 nm, the crystal was exchanged for a longer 10 mm periodically poled lithium tantalate crystal (HC Photonics) that provided higher gain [11]. The outcoupled signal pulses were dechirped using a simple pair of 150 lines/mm reflective gratings with 5–10 cm separation. The total compressor losses were ∼60%, as we used readily available gratings with no optimization. These losses could be reduced by using optimized transmissive gratings or chirped mirrors. When optimizing the measurements in Fig. 2(a) with the compressor for shortest pulses, we were able to dechirp the signal below 38 fs (assuming Gaussian shape), which is more than five times shorter than the pump pulse duration. Figure 3 shows the wavelength-tunable sub-38 fs pulses covering the 1.2–2 μm spectral region. Even though the optimized pulses were close to the duration of their Fourier transform limit (31–34 fs), better compression could be achieved by compensating the third-order dispersion that was added by the grating compressor. In this case, using optimized chirped mirrors may provide better dispersion compensation and lower losses.

In addition to its main advantage in compactness, this fiber-feedback design forces the OPO to operate in a highly dispersed regime, resulting in a strongly chirped signal pulse. The FF has a
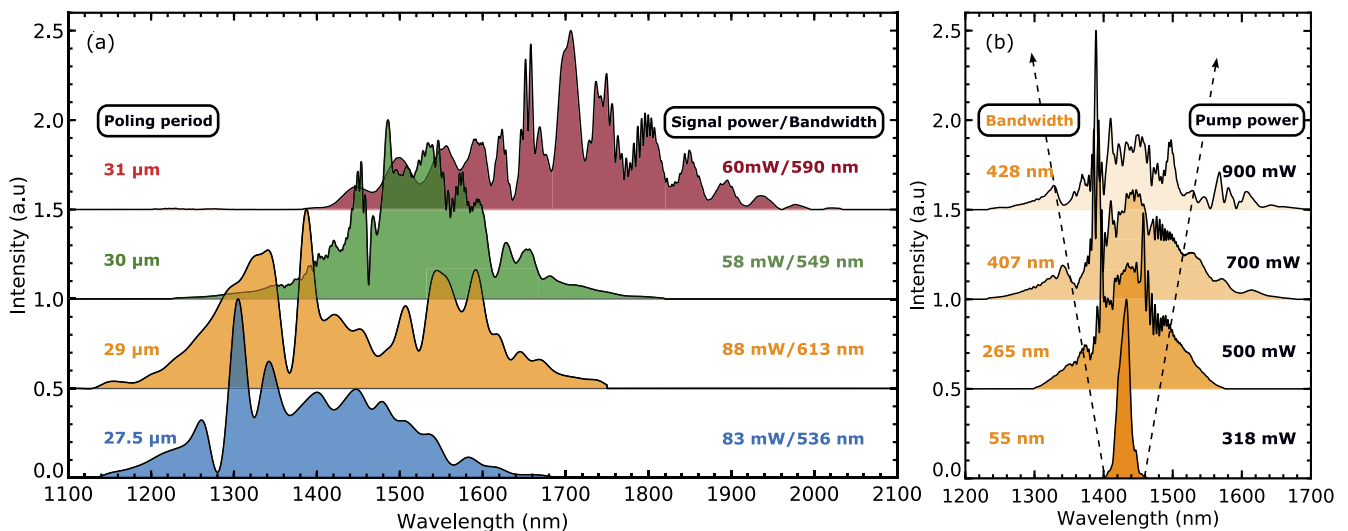

Fig. 2. Broadband and tunable spectra achieved by combining $\chi^{(2)}$ nonlinearity in periodically poled crystals and $\chi^{(3)}$ nonlinearity in the FF. (a) Tunability of broadband spectra spanning 1100–2000 nm spectral region using different poling periods (27–31 μm) in the nonlinear crystal. (b) Controlled spectral broadening after the nonlinear FF for fixed poling period (29 μm) by increasing the pump power. All spectra are in linear scale and shifted upward by 0.5 step for clarity. The dotted arrows in (b) are guide to the eye.
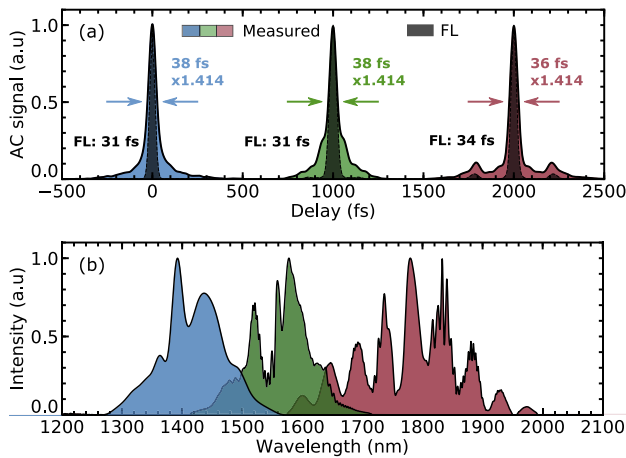
Fig. 3. Dechirped sub-40 fs pulses spanning from 1.2 to 2 µm. (a) Autocorrelation signals for the compressed output beam at different poling periods. (b) Corresponding spectrum. The auto-correlations are shifted by 1000 fs for clarity and the dark shaded regions represent the calculated Fourier limit (FL).

Fig. 4. Passive stability of free-running operation for 2 h. (a) Power stability of the pump and signal at comparable power levels. Inset: 1 mW range of the signal power, demonstrating 79 µW standard deviation. (b), (c) 30 spectra/min were recorded with 0.04% rms drift of the central wavelength. The solid line in (b) is the average spectrum, whereas the shaded area shows the maximum spectral deviation over the entire measurement.

round-trip group delay dispersion (GDD) of 0.04 ps^2 at 1.55 µm [17]. As a result, the circulating intracavity signal is expected to reach ~0.8 ps after one round trip, owing to GDD in the fiber; when combined with the spectral and temporal broadening provided by SPM, the intracavity pulse reaches ~3 ps pulse duration. The available fiber was not polarization maintaining (PM); to minimize any birefringence, we stretched the fiber, avoiding any twisting. Therefore, in this operation regime, the synchronization with the 200-fs pump pulse becomes insensitive to cavity length mismatch from either mechanical or thermal fluctuations. This results in a less sensitive tunability of 0.1–0.2 nm/µm, in comparison with 3 nm/µm for conventional free-space OPOs [6]. Furthermore, by decoupling the parametric gain from gain bandwidth, taking advantage of SPM in the FF, we were able to operate the OPO in a high-gain regime using longer nonlinear crystals (5–10 mm) with large outcoupling ratio (80–95%). This resulted in excellent insensitivity to losses (~80%) [8] compared with other systems when 0.25–1 mm crystals were used to provide sufficient gain bandwidth [6,10,12,18]. To demonstrate the stability of the system, and to use the same power meter, the pump power was reduced to a comparable level as the signal using a reflection from a sapphire plate. We recorded the free-running signal power and spectrum at 1400 nm for 2 h (see Fig. 4). The signal power instability was 0.09% rms within a fluctuation window of only 79 µW (Fig. 4(a)). In Fig. 4(b), the spectral stability is shown with central wavelength fluctuation of only 0.04% rms. During this time, the system was not housed and there was no kind of stabilization, even to the laboratory temperature. This SPM-enhanced operation demonstrates excellent and completely passive stability, higher than previously reported in fiber-feedback OPOs [11,12]. We attribute this outstanding stability to strong intracavity dispersion paired with operation of the OPO FF in the normal dispersion regime. This avoids soliton dynamics and modulation instability [12,19].

In conclusion, we present a simple, compact, and robust sub-38 fs OPO, which is five times shorter than the 200-fs pump at 1030 nm. The OPO is tunable in the near-IR spectral region 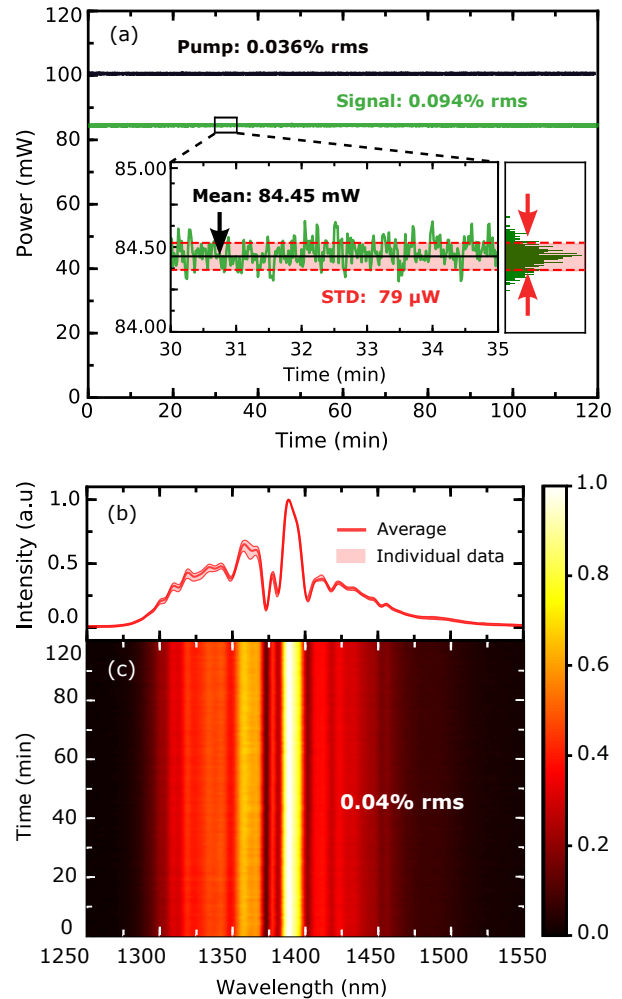across 1.1–2 µm, with outstanding passive power and spectral stability below 0.094% rms and 0.04%, respectively. Exploiting $\chi^{(2)}$ in a nonlinear crystal and $\chi^{(3)}$ in a normal dispersion FF, we demonstrated coherent and controllable broadening up to a bandwidth of 600 nm (−20 dB), with up to 90 mW signal power. We attribute the excellent passive stability to the high intracavity normal dispersion paired with strong SPM broadening, which resulted in a highly chirped 3 ps intracavity signal pulse insensitive to pump-signal overlap. Additionally, by decoupling the signal spectral bandwidth from the parametric gain, we operated the OPO in a high-gain regime using long nonlinear crystal (5–10 mm) with high outcoupling ~90%, resulting in unusual insensitivity to losses and ambient fluctuations [8,11]. Importantly, the use of intracavity fiber reduces the required optics and enables a footprint of only 14 × 14 cm^2, resulting in an ultracompact and cost-effective source. All components used are commercially available, making our system reproducible and reliable, with outstanding passive free-running stability and no active stabilization electronics. This fiber-feedback OPO is a practical source for various applications, such as time-resolved

ultrafast spectroscopy and multiphoton imaging. Finally, few-cycle pulses are feasible using commercially available, highly nonlinear fibers with near-zero normal dispersion. This allows a coherent octave broadening with compressible chirp to the single-cycle regime [20].

Disclosures. The authors declare no conflicts of interest.

Data availability. Data underlying the results presented in this paper are not publicly available at this time but may be obtained from the authors upon reasonable request.

REFERENCES

1. R. L. Fork, C. H. Brito Cruz, P. C. Becker, and C. V. Shank, Opt. Lett. **12**, 483 (1987).
2. R. Ell, U. Morgner, F. X. Kärtner, J. G. Fujimoto, E. P. Ippen, V. Scheuer, G. Angelow, T. Tschudi, M. J. Lederer, A. Boiko, and B. Luther-Davies, Opt. Lett. **26**, 373 (2001).
3. D. H. Sutter, G. Steinmeyer, L. Gallmann, N. Matuschek, F. Morier-Genoud, U. Keller, V. Scheuer, G. Angelow, and T. Tschudi, Opt. Lett. **24**, 631 (1999).
4. G. Krauss, S. Lohss, T. Hanke, A. Sell, S. Eggert, R. Huber, and A. Leitenstorfer, Nat. Photonics **4**, 33 (2010).
5. J. Hebling, X. P. Zhang, H. Giessen, J. Kuhl, and J. Seres, Opt. Lett. **25**, 1055 (2000).
6. S. Chaitanya Kumar, A. Esteban-Martin, T. Ideguchi, M. Yan, S. Holzner, T. W. Hänsch, N. Picqué, and M. Ebrahim-Zadeh, Laser Photonics Rev. **8**, L86 (2014).
7. J. Heng, P. Liu, and Z. Zhang, Opt. Express **28**, 16740 (2020).
8. T. Sudmeyer, J. Aus Der Au, R. Paschotta, U. Keller, P. G. Smith, G. W. Ross, and D. C. Hanna, J. Phys. D: Appl. Phys. **34**, 2433 (2001).
9. F. Kienle, P. Siong Teh, S.-U. Alam, C. B. E. Gawith, D. C. Hanna, D. J. Richardson, and D. P. Shepherd, Opt. Lett. **35**, 3580 (2010).
10. K. A. Ingold, A. Marandi, M. J. F. Digonnet, and R. L. Byer, Opt. Lett. **40**, 4368 (2015).
11. T. Steinle, F. Moerz, A. Steinmann, and H. Giessen, Opt. Lett. **41**, 4863 (2016).
12. C. F. O'Donnell, S. C. Kumar, T. Paoletta, and M. Ebrahim-Zadeh, Optica **7**, 426 (2020).
13. P. Yin, J. R. Serafini, Z. Su, R.-J. Shiue, E. Timurdogan, M. L. Fanto, and S. Preble, Opt. Express **27**, 24188 (2019).
14. H. Linnenbank, T. Steinle, F. Mörz, M. Flöss, H. Cui, A. Glidle, and H. Giessen, Adv. Photonics **1**, 055001 (2019).
15. Z. Zhang, J. Sun, T. Gardiner, and D. T. Reid, Opt. Express **19**, 17127 (2011).
16. C. Manzoni and G. Cerullo, J. Opt. Soc. Am. B **18**, 103501 (2016).
17. P. Ciąćka, A. Rampur, A. Heidt, T. Feurer, and M. Klimczak, J. Opt. Soc. Am. B **35**, 1301 (2018).
18. R. A. McCracken and D. T. Reid, Opt. Lett. **40**, 4102 (2015).
19. B. Sierro, P. Hänzi, D. Spangenberg, A. Rampur, and A. M. Heidt, Optica **9**, 352 (2022).
20. D. M. Lesko, H. Timmers, S. Xing, A. Kowligy, A. J. Lind, and S. A. Diddams, Nat. Photonics **15**, 281 (2021).